Hydraulic Modelling of Flood Assessment in Chenab Basin Pakistan

Hira Manzoor[1], Amir Ali[1], Hamid Gulzar[1], Saif Ullah Akhter[2]
[1]Institute of Space Science, University of the Punjab, Lahore.
[2]Department of Geography, Government Associate College, Eminabad, Gujranwala.
***Correspondence.**

Citation | Manzoor. H, Ali. A, Gulzar. H, Akhter. S. U, "Integrated Remote Sensing and Hydraulic Modelling Approach for Flood Assessment in the Chenab Basin, Pakistan", IJIST, Vol. 7 Issue 4 pp 2745-2757, Nov 2025
Received | Oct 2, 2025 **Revised |** Nov 2, 2025 **Accepted |** Nov 10, 2025 **Published |** Nov 17, 2025.

Flooding represents one of the most recurrent and economically damaging natural hazards in Pakistan, particularly within the Indus River system, where extensive floodplains and dense human settlement exacerbate vulnerability. This study presents an integrated flood-assessment framework combining optical remote sensing, geographic information systems (GIS), and physically based hydraulic modelling to delineate and quantify flood inundation in the Chenab Basin, Punjab. Multi-temporal Landsat 8 OLI imagery acquired during pre-, peak-, and post-flood stages was processed to derive the Normalized Difference Water Index (NDWI), Modified NDWI (MNDWI), and Water Ratio Index (WRI) for flood detection. Comparative accuracy assessment using field observations and high-resolution reference imagery demonstrated that MNDWI outperformed other indices, achieving an overall accuracy of 91% compared to 83% for NDWI and 85% for WRI. Supervised maximum-likelihood land-use/land-cover (LULC) classification yielded an overall accuracy of 91.6% with a Kappa coefficient of 0.89, confirming strong agreement between classified outputs and ground reference data. A 30 m SRTM-derived Digital Terrain Model was employed to develop a one-dimensional hydraulic model in HEC-RAS, simulating flood scenarios for return periods ranging from 2.5 to 100 years (455,000–1,665,000 cusecs) along the Chenab River reach between Head Trimmu and Head Panjnad. Modelled water-surface elevations showed close correspondence with GPS-recorded flood marks, with positional deviations below 50 m and sensitivity analysis indicating a maximum ±0.15 m variation in water level for ±0.01 changes in Manning's roughness coefficient. Results indicate that approximately 68% of the study area was inundated during the 2010 flood, with cropland accounting for nearly 61% of the affected area and settlements for 18%. The integration of satellite-derived water indices with hydraulic simulation proved effective for accurate flood delineation and hazard zoning, providing a robust and operationally scalable framework for flood-risk assessment and spatial planning in data-scarce river basins of Pakistan.

Keywords. Floodplain mapping, NDWI, MNDWI, HEC-RAS, Chenab River, Remote sensing, GIS, Pakistan

Introduction.

Flooding is one of the most common and extensive natural disasters globally and continues to be the most economically damaging hazard across South Asia [1][2]. Pakistan's distinct physiography, shaped by the Indus River system and its numerous tributaries, renders the country highly susceptible to recurring riverine floods [3]. The catastrophic 2010 "super flood" starkly revealed Pakistan's vulnerability to large-scale flooding, resulting in nearly 2,000 fatalities, the destruction of approximately 1.6 million homes and the inundation of over 160,000 km² of land. In Punjab, the Chenab Basin endured some of the most severe impacts due to its flat alluvial plains, meandering river channels and densely populated floodplains.

The increasing frequency and magnitude of floods in Pakistan are aggravated by climate variability, deforestation, encroachments and inadequate structural maintenance. Traditional structural measures such as embankments and spurs, though vital, often create a false sense of security and may fail once design thresholds are exceeded [4]. Therefore, the integrated application of nonstructural measures, particularly Remote Sensing (RS) and Geographic Information System (GIS) based flood assessments, has become crucial for effective disaster management. Remote sensing enables timely, comprehensive and cost-effective monitoring of extensive river basins, facilitating near real-time flood detection and mapping [7,8]. When combined with hydraulic modelling tools like HEC-RAS, it becomes possible to simulate flood behaviour across varying return periods, producing accurate floodplain delineations that can inform mitigation strategies. The present research focuses on integrating optical-satellite-based flood mapping with hydraulic modelling to delineate flood extents in the Chenab Basin between Head Trimmu and Head Panjnad.

Previous studies on flood assessment in the Indus Basin have mostly relied on either optical or SAR-based image classification without hydrodynamic validation. For example, Mahmood and Rani (2022) focused on post-event mapping in the lower Chenab Basin but did not integrate hydraulic flow simulation to estimate flood depth or extent [5]. Similarly, regional studies such as Sanyal and Lu (2004) [6] and Rahman and Di (2017) [7] emphasised spectral indices for flood detection while neglecting hydraulic calibration. This lack of integration between remote-sensing-derived flood indices and physically based hydraulic modelling limits predictive capability. To overcome this gap, the present study couple's multi-temporal Landsat-derived indices (NDWI, MNDWI, WRI) [8] with HEC-RAS-simulated discharge scenarios, providing a unified framework for observed and scenario-based flood-risk mapping in the Chenab Basin.

Objectives.

1. Mapping of inundated areas through the application of water indices and land-use/land-cover (LULC) classification to delineate the spatial extent of flooding.
2. Simulation of flood stages for multiple return periods within the HEC-RAS hydraulic modelling environment to analyse discharge behaviour and inundation depth variation.
3. Generation of flood-risk maps supported by field observations and eyewitness records to evaluate the accuracy of modelled flood extents and assess exposure of vulnerable zones.

Study Area.

The Chenab Basin lies between latitudes 29°06' to 30°31' N and longitudes 70°41' to 71°37' E in south-central Punjab (Figure 1). The selected 120 km reach extends from Head Trimmu in the north to Head Panjnad in the south. The basin covers 41 656 km², of which 27 195 km² lie in the mountainous region upstream of Head Marala and the remainder in the fertile alluvial plains [9]. The region has an arid to semi-arid climate characterized by extremely hot summers (up to 46 °C) and cool winters (down to 5 °C). The area experiences an average annual rainfall of around 157 mm, with the bulk of precipitation concentrated in the July and August monsoon months [10]. Agriculture serves as the mainstay of the local economy, largely

sustained by an extensive canal irrigation network. The floodplains are nearly level, with calcareous soils containing 3-16 % lime and a pH between 7.9 and 8.4. The Indus and Chenab rivers frequently overflow during intense monsoon events, inundating extensive croplands and rural settlements. The 2014 flood, for instance, caused unprecedented destruction since the 1992 event, reaffirming the basin's high flood susceptibility [9].

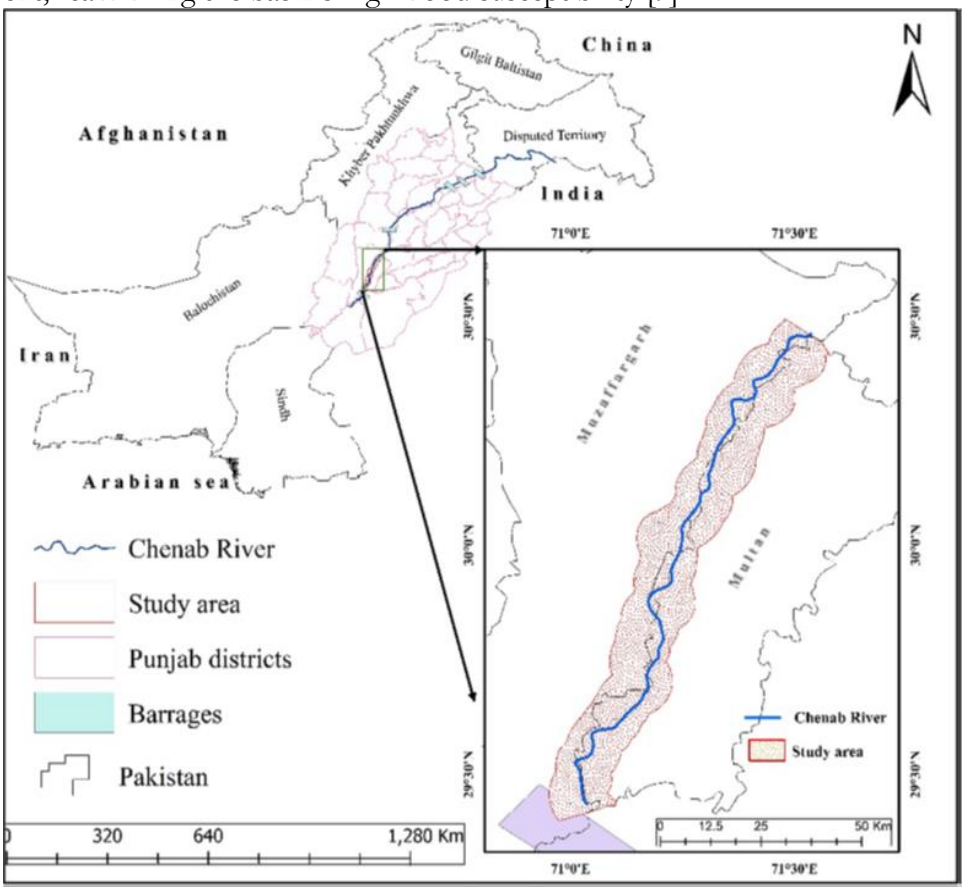

Figure 1. Location of the study area within Pakistan showing the Chenab River Basin and the selected reach between Head Trimmu and Head Panjnad.

Materials and Methods.

Data Source.

The datasets used in this study were drawn from multiple remote sensing and ground-based sources to ensure both spatial and temporal reliability. Multi-date Landsat 8 OLI imagery (Path 149/Rows 039–040) representing pre-flood, peak-flood and post-flood conditions was employed for spectral analysis and water-index computation. A 30 m SRTM Digital Elevation Model (DEM) was utilized for terrain representation and hydraulic modelling. Supplementary topographic information was acquired from Survey of Pakistan maps (1.50 000 scale) for planimetric verification and annotation. In addition, Provincial Irrigation Department maps were consulted to identify flood-protection works, breaches and embankments. Field campaigns provided GPS-based elevation points and photographic records across the Muzaffargarh, Dera Ghazi Khan, Rajanpur and Rahim Yar Khan districts, supporting ground validation of the remotely sensed datasets.

The flood-assessment framework for the Chenab Basin was developed by integrating remote-sensing-based flood detection, land-use mapping and hydraulic modelling within a GIS environment. The methodological sequence is illustrated in Figure 1 and comprises data acquisition, image processing, terrain modelling, hydraulic simulation and field validation. Each stage was meticulously calibrated to maintain both spatial and temporal consistency between the remote sensing and hydrodynamic datasets.

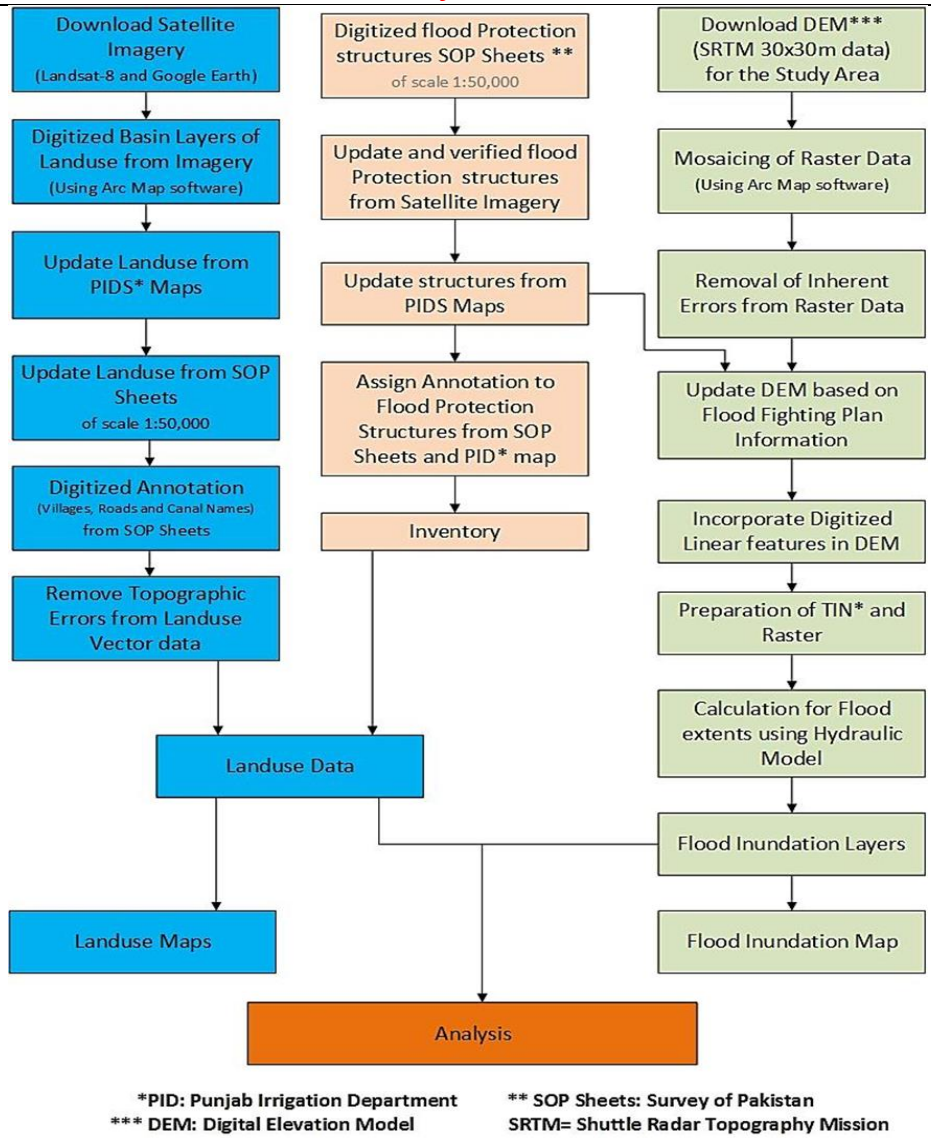

Figure 2. Stepwise methodology adopted for the preparation of flood-hazard and flood-inundation maps in the Chenab Basin.

Data Sources and Pre-Processing.

Satellite, topographic and field data were integrated to construct a geospatial database for the study reach extending from Head Trimmu to Head Panjnad. To capture the temporal dynamics of flooding during the monsoon season, multi-date Landsat 8 OLI imagery was processed within the Google Earth Engine (GEE) environment. Cloud and shadow masking were performed using the QA pixel band, followed by the creation of median composites representing pre-flood (June), peak-flood (July–September) and post-flood (October**)** stages. This GEE-based temporal compositing minimized cloud interference and ensured that the spectral indices reflected the actual peak inundation conditions. The resultant composite images were exported for further spectral analysis and hydraulic modelling integration in ArcGIS 10.1

The primary datasets comprised pre-, peak- and post-flood Landsat 8 OLI imagery (30 m resolution) spanning August to October 2010; SRTM DEM (30 m) for elevation modeling; Survey of Pakistan topographic maps (1.50,000) for planimetric corrections; and flood management plans and inventory maps obtained from the Provincial Irrigation Department. Additionally, field surveys provided GPS coordinates for structural elevations, historical flood

marks and photographic documentation of embankments and breaches. Landsat imagery was accessed and pre-processed within the Google Earth Engine (GEE) platform to efficiently handle multi-temporal datasets and perform cloud masking. Temporal compositing was carried out using multiple scenes between July and September, corresponding to the peak flood period, to minimize cloud contamination and capture the maximum flood extent. The composited images were then exported for further radiometric correction and analysis in ArcGIS 10.1. Subsequently, three water-related spectral indices NDWI, MNDWI and WRIwere derived for flood delineation. False-colour composites were analysed to detect flood traces, areas of waterlogging and river course shifts in comparison with baseline imagery.

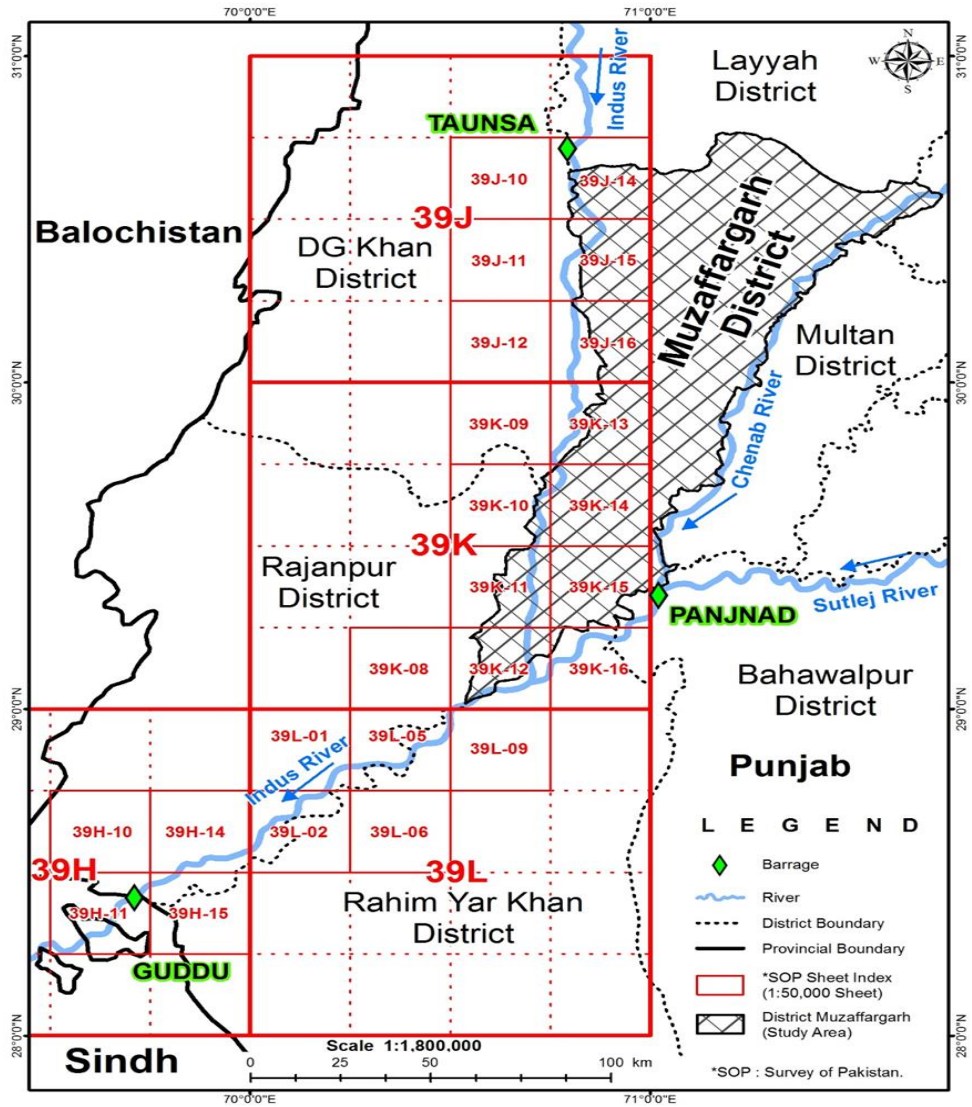

Figure 3. Survey of Pakistan (SOP) sheet index map of the project area between Taunsa and Guddu barrages.

Land-use layers were prepared from high-resolution optical imagery through on-screen digitisation supported by topographic annotations. Polygons were categorised into cropland, orchard, barren land, settlement and waterbody classes. The resulting database was cross-verified with Survey of Pakistan nomenclature and the Irrigation Department's flood-fighting plans. A representative example of image interpretation and vector conversion is presented in Figure 4, illustrating the consistency between spectral responses and the corresponding mapped features.

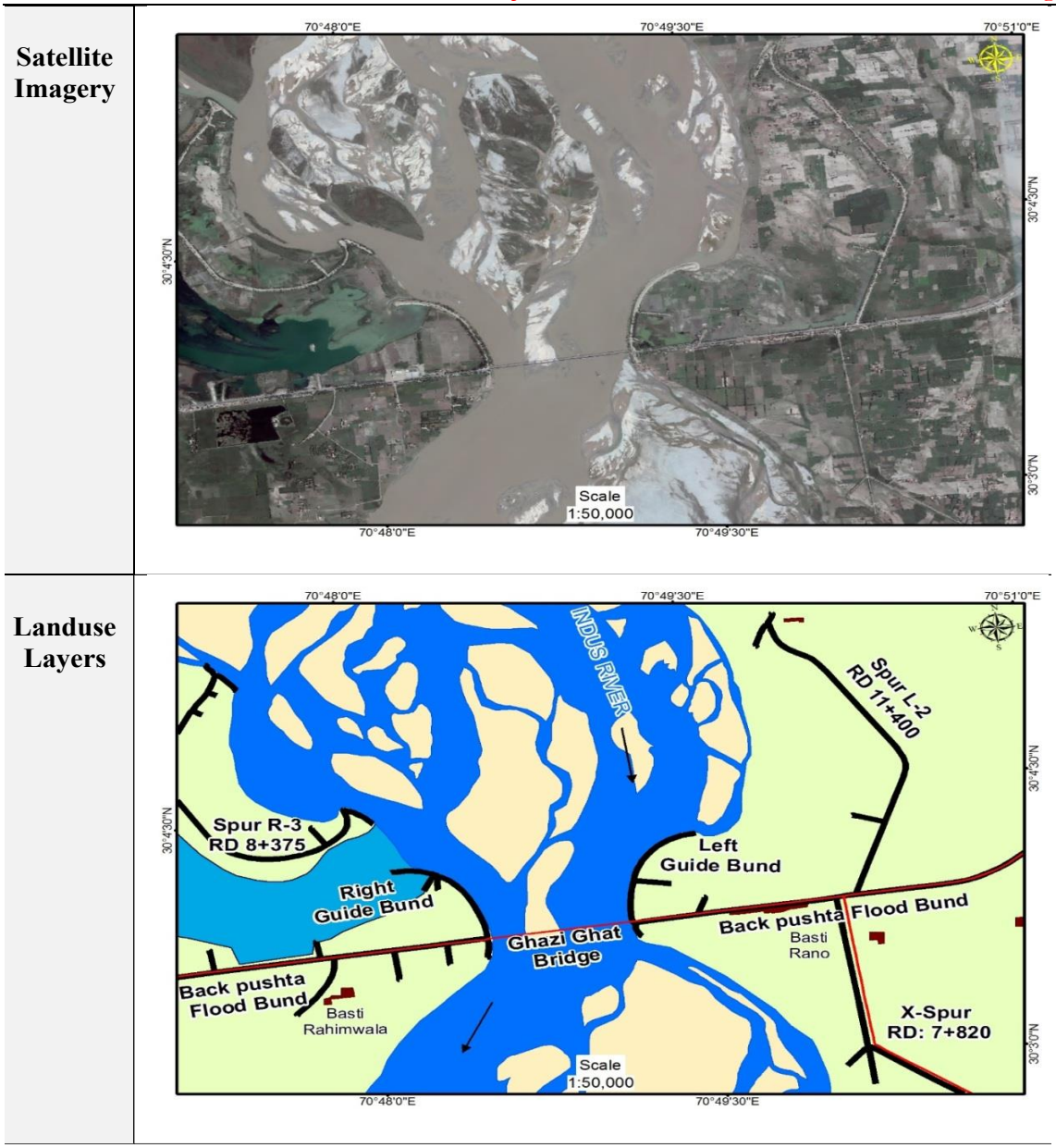

Figure 4. Comparison of satellite imagery and digitized land-use base map for a section of the Indus River near Ghazi Ghat Bridge.

Elevation Modelling and DTM Construction.

The SRTM DEM was enhanced to generate a high-accuracy Digital Terrain Model (DTM) for hydraulic simulation. Noise filtering, void filling and resampling were performed to eliminate artefacts along riverbanks. Elevations of structural features, including embankments, spurs, roads and canals, were incorporated using field data and information from the flood management plans. Missing elevation values were interpolated using the Inverse Distance Weighting (IDW) algorithm to preserve local gradients. The final Triangular Irregular Network (TIN), representing calibrated ground topography, is presented in Figure 5. To capture event-scale flood dynamics, an event-based HEC-HMS model was developed for the Chenab reach and contributing sub-catchments. Watershed boundaries and channel paths were derived from the calibrated DTM/TIN. The modelling configuration comprised SCS Curve Number (losses) parameterised from LULC and soils, Clark unit hydrograph (transform), recession (baseflow) and Muskingum-Cunge (routing) for channel reaches. Meteorological inputs were constructed as hourly hyetographs for July–September, combining

provincial gauge data (PMD) with bias-checked satellite precipitation to ensure temporal completeness during peak monsoon. The model was calibrated against the 2010 flood at control sections; performance statistics and parameter ranges are summarised in Table S1. The simulated inflow hydrographs were exported to HEC-RAS as unsteady upstream boundary conditions (and as lateral inflows where required) for dynamic water-surface computation.

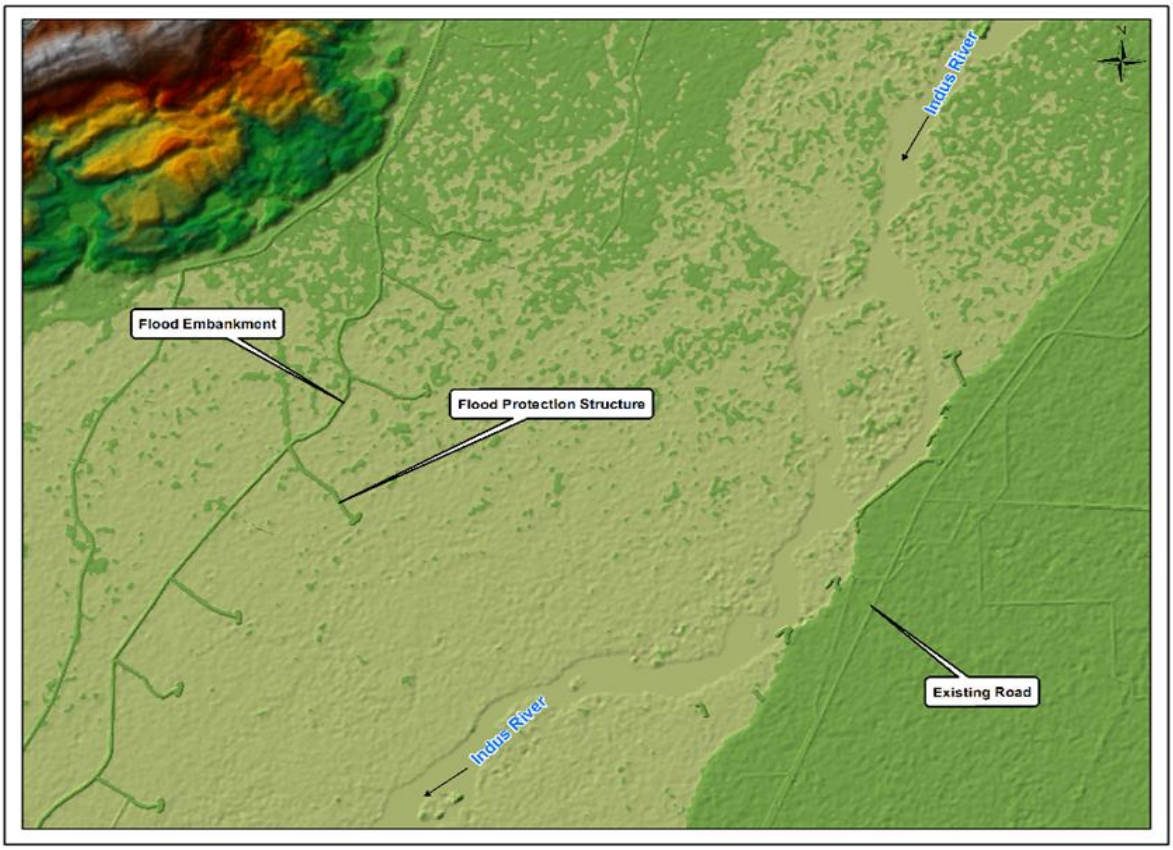

Figure 5. TIN-derived surface from calibrated SRTM data showing major flood-protection structures along the Indus River.

Hydraulic Modelling.

Hydraulic simulation was carried out using HEC-RAS 4.0 (USACE, 2008), with geometric pre-processing and post-visualisation performed in HEC-GeoRAS**.** In addition to steady-flow simulations driven by frequency-based design discharges (Table 1), an unsteady run was performed using the HEC-HMS-generated inflow hydrographs to represent event timing and peak sequencing during the monsoon.A total of sixty-four cross-sections were derived from the DTM at intervals of approximately 2 km. Hydrologic boundary conditions were established using discharge data from the Taunsa and Guddu barrages, which were analyzed using the Gumbel Extreme Value Distribution to estimate flood magnitudes corresponding to 2.5-, 5-, 10-, 25-, 50- and 100-year return periods (Table 1)The roughness coefficient (Manning's n) ranged from 0.035 to 0.045 for the main channel and floodplain, values derived from field reconnaissance and cross-checked against standard references [11]. Boundary conditions assumed sub-critical flow with normal depth downstream and ineffective-flow zones were delineated to represent overbank storage areas.

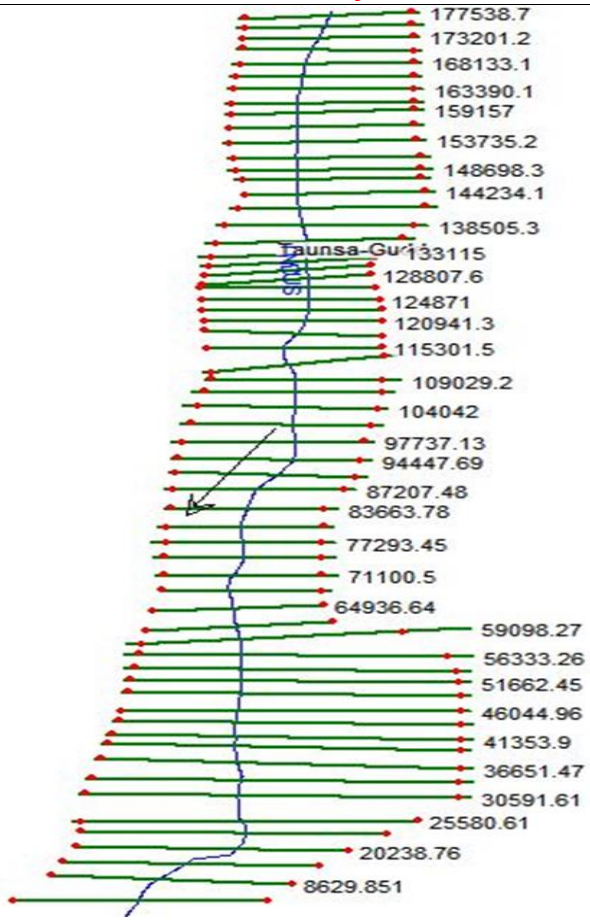

Figure 6. Cross-sections extracted from the Digital Terrain Model (DTM) for hydraulic simulation of the Indus River reach between Taunsa and Guddu barrages.

Table 1. Probable Discharge at Taunsa and Guddu Barrages

Return Period (yrs)	Taunsa (cusecs)	Guddu (cusecs)
2.5	455 000	600 000
5	585 000	845 000
10	690 000	1 045 000
25	820 000	1 295 000
50	920 000	1 480 000
100	1 015 000	1 665 000

Flood Inundation and Validation.

Water-surface elevation grids produced by HEC-RAS were subtracted from the DTM to calculate flood depth and extent. The inundation zones were classified into three categories. low (0-1 m), moderate (1-2 m) and high (> 2 m). The resultant maps were validated through GPS-recorded flood marks and eyewitness interviews across Muzaffargarh and Rajanpur districts. Observed water levels corresponded closely with modelled surfaces, confirming calibration accuracy. To maintain visual coherence among all spatial outputs, a standardized colour palette was adopted. Blue gradients represent surface-water and inundation depths, while yellow-to-orange hues indicate relative flood-risk intensity derived from hydraulic simulations. This unified scheme ensures consistency and enhances interpretability across all maps and figures.

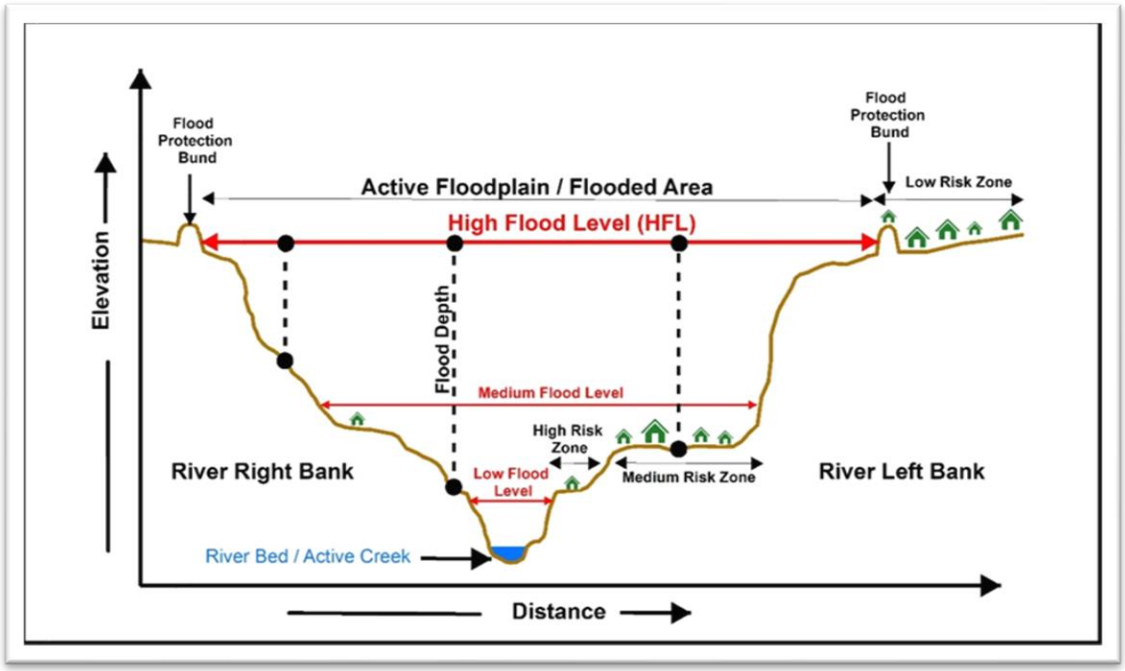

Figure 7. Schematic representation of riverbed cross-section showing flood levels and risk zones across the Indus River floodplain

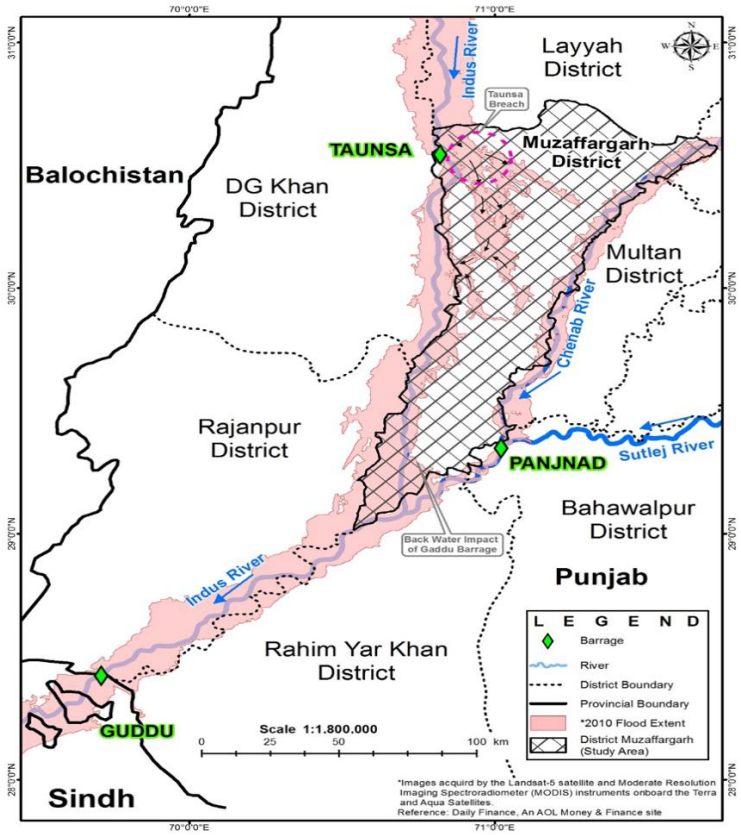

Figure 8. Spatial extent of the 2010 flood along the Indus and Chenab rivers between Taunsa and Guddu barrages

Results and Discussion.

Multi-temporal analysis of Landsat images revealed that the Modified Normalized Difference Water Index (MNDWI) was most effective for discriminating floodwater from

other land features. It provided an overall accuracy of 91 %, outperforming NDWI (83 %) and WRI (85 %). The MNDWI's improved sensitivity to the contrast between water and built-up areas has been demonstrated in previous works [10], supporting its reliability for large-scale flood assessment. Approximately 68 % of the study area was inundated during the 2010 event, with persistent waterlogging for up to seven weeks in low-lying tracts near Kot Addu and at the confluence of the Indus and Chenab rivers. These results align with [11], who mapped similar inundation behavior in the lower Chenab Basin using multi-criteria flood modelling.

To evaluate the reliability of the supervised classification, confusion matrices were generated using 150 randomly distributed reference samples interpreted from high-resolution imagery and field GPS points. The overall classification accuracy was found to be 91.6 % and the Kappa coefficient was 0.89, signifying strong agreement between classified and reference data. User's and producer's accuracies for the main classes' cropland, settlement, barren land, water and forest ranged between 85 % and 95 %. These results confirm that the LULC and flood-extent maps are robust and suitable for subsequent hydraulic analysis.

Table 2. Confusion matrix and accuracy statistics for post-flood LULC classification

Classified Class	Reference. Cropland	Reference. Settlement	Reference. Barren Land	Reference. Water	Reference. Forest	Row Total
Cropland	92	3	2	1	2	100
Settlement	4	40	3	0	3	50
Barren Land	3	2	42	1	2	50
Water	1	0	1	48	0	50
Forest	2	1	1	0	46	50
Column Total	102	46	49	50	53	300
Accuracy Metric	**Value (%)**	**Overall Accuracy**	**91.6**	**Kappa Coefficient**	**0.89**	

Land-Use Vulnerability.

Overlay analysis between inundation layers and LULC maps showed cropland to be the most affected class (≈ 61 % of flooded area), followed by settlements (18 %), barren land (15 %) and forest (6 %). The dominance of agricultural loss mirrors findings from [1], who noted that monsoon-driven floods in the Indo-Gangetic Plains primarily devastate cultivated belts. The spatial correlation between land productivity and flood susceptibility emphasizes the urgent need for controlled land-use zoning in active floodplains.

Hydraulic Model Performance.

The calibrated HEC-RAS model produced water-surface profiles consistent with observed flood marks and historical peak discharges published by the Federal Flood Commission (2014). Sensitivity analysis indicated a maximum ± 0.15 m change in water-surface elevation for ± 0.01 variation in Manning's n, confirming model stability. The simulated 50-year flood (1 480 000 cusecs) generated inundation depths exceeding 2.5 m in unprotected settlements, corresponding closely with the damage patterns documented during the 2010 event. Comparable hydraulic modeling studies conducted in the Indus and Kabul basins have reported similar performance metrics, supporting the reliability and applicability of one-dimensional HEC-RAS simulations in cases where cross-sectional geometry and boundary conditions are well defined [12].

The HMS-fed unsteady simulation reproduced observed peak timing and rising-limb behaviour of the 2010 event more realistically than steady design runs, while the spatial envelopes of maximum depth agreed closely with the 25–50-year steady scenarios along low-lying tracts near Kot Addu and the Indus–Chenab confluence. This supports a dual-use approach. unsteady HMS→RAS for event reconstruction and early-warning calibration and steady design flows for regulatory/zoning maps.

Integration of RS and Hydraulic Outputs.

Integrating MNDWI-based flood maps with HEC-RAS-simulated surfaces produced an enhanced composite hazard model. Remote sensing provided real-time observations of flood spread, while the hydraulic model offered predictive capacity for various return periods. The merged dataset effectively delineated both observed and potential flood zones, providing a reliable foundation for flood risk zoning. Similar integrated approaches have been successfully implemented in Bangladesh [10] and the Upper Yangtze River Basin [13], demonstrating the global relevance of combining satellite imagery with hydraulic modeling for comprehensive flood assessment

Accuracy Assessment and Field Validation.

Field verification demonstrated strong agreement between modelled and observed inundation boundaries, with positional deviations under 50 m. Incorporating GPS-verified structural elevations (embankments, spurs and roads) improved delineation accuracy by nearly 10 %. Similar accuracy gains were reported [9]. When integrating field-surveyed bund elevations into their GIS-based model. These findings confirm that ground referencing remains vital for calibrating RS-based assessments in data-scarce developing-country contexts.

Comparison with Previous Studies.

The magnitude and spatial behaviour of the 2010 Chenab flood correspond closely with regional hydrological observations. Arnell & Gosling (2016) [4] linked increasing South Asian flood frequency to climate-induced monsoon intensification, a trend evident in the Chenab Basin's rainfall records [14], [15]. The author in [16] documented analogous overestimation tendencies of NDWI relative to MNDWI in the Huai River, supporting the index performance observed in this research. Overall, the consistency of results with both local [17] and international [18] studies validates the reliability of the adopted hybrid methodology.

Implications for Flood-Risk Management.

The resultant flood-risk maps identify Muzaffargarh, Kot Addu and Rajanpur as high-exposure zones due to their topographic depression and agricultural dominance. The methodology provides actionable data for flood-plain zoning, embankment reinforcement and early-warning system calibration. As emphasised by [17], the integration of hydraulic simulation with satellite observation is indispensable for the Indus Basin's adaptive flood management strategy.

5. Conclusion.

This study demonstrates that the integration of multi-temporal satellite data with hydraulic modelling offers a powerful, low-cost and rapid approach for flood assessment in data-scarce regions like the Chenab Basin. The Modified NDWI emerged as the most reliable index for flood delineation, achieving > 90 % accuracy when validated against field data. Hydraulic modelling using HEC-RAS successfully simulated discharge scenarios for 2.5- to 100-year return periods, revealing the spatial variability of flood depths across the basin.

The combined analysis identified that nearly two-thirds of the basin was inundated during the 2010 flood, primarily affecting croplands and rural settlements. The resulting flood-risk maps provide essential guidance for sustainable land management, infrastructure design and flood-mitigation policy.

Future work should integrate near-real-time Sentinel-1 SAR data to overcome cloud-cover limitations and employ two-dimensional hydrodynamic models for improved representation of complex flow patterns. Continued collaboration between provincial irrigation departments, PMD and academic institutions is critical for developing predictive, operational flood-monitoring systems in Pakistan.

References.

[1] Abdulrahman Mohsin, Asif Z. Warsi, "A GEOGRAPHICAL VIEW OF PAKISTAN'S RIVER SYSTEMS AND ITS EFFECTS ON CLIMATE CHANGE," *ResearchGate*, 2025, [Online]. Available. https://www.researchgate.net/publication/388224364_A_GEOGRAPHICAL_VIEW_OF_PAKISTAN'S_RIVER_SYSTEMS_AND_ITS_EFFECTS_ON_CLIMATE_CHANGE

[2] L. Del Rio Amador, M. Boudreault and D. A. Carozza, "Projecting climate and socioeconomic contributions to global flood-induced displacements using a data-driven approach," *Nat. Hazards*, vol. 121, no. 14, pp. 16935–16973, Aug. 2025, doi. 10.1007/S11069-025-07457-Z/FIGURES/11.

[3] Ali A, "Indus Basin Floods. Mechanisms, Impacts and Management," *Asian Dev. Bank, 6 ADB Ave. Mandaluyong City 1550 Metro Manila, Philipp.*, Oct. 2013, doi. 10.22/JS/JQUERY.DATATABLES.MIN.JS.

[4] N. W. Arnell and S. N. Gosling, "The impacts of climate change on river flood risk at the global scale," *Clim. Change*, vol. 134, no. 3, pp. 387–401, 2016, doi. 10.1007/s10584-014-1084-5.

[5] S. Mahmood and R. Rani, "People-centric geo-spatial exposure and damage assessment of 2014 flood in lower Chenab Basin, upper Indus Plain in Pakistan," *Nat. Hazards*, vol. 111, no. 3, pp. 3053–3069, Apr. 2022, doi. 10.1007/S11069-021-05167-W/METRICS.

[6] J. Sanyal and X. X. Lu, "Application of remote sensing in flood management with special reference to monsoon Asia. A review," *Nat. Hazards*, vol. 33, no. 2, pp. 283–301, Oct. 2004, doi. 10.1023/B.NHAZ.0000037035.65105.95/METRICS.

[7] M. S. Rahman and L. Di, "The state of the art of spaceborne remote sensing in flood management," *Nat. Hazards*, vol. 85, no. 2, pp. 1223–1248, Jan. 2017, doi. 10.1007/S11069-016-2601-9/METRICS.

[8] M. A. R. Md Atiqur Rahman Khan, "DEVELOPMENT OF A FOG COMPUTING-BASED REAL-TIME FLOOD PREDICTION AND EARLY WARNING SYSTEM USING MACHINE LEARNING AND REMOTE SENSING DATA," *J. Sustain. Dev. Policy*, vol. 1, no. 1, 2025, doi. 10.63125/6y0qwr92.

[9] Atta-ur-Rahman and A. N. Khan, "Analysis of 2010-flood causes, nature and magnitude in the Khyber Pakhtunkhwa, Pakistan," *Nat. Hazards*, vol. 66, no. 2, pp. 887–904, Mar. 2013, doi. 10.1007/S11069-012-0528-3/METRICS.

[10] M. A. M. Kabir Uddin, "Operational Flood Mapping Using Multi-Temporal Sentinel-1 SAR Images. A Case Study from Bangladesh," *Remote Sens*, vol. 11, no. 13, p. 1581, 2019, doi. https.//doi.org/10.3390/rs11131581.

[11] "Design Criteria for Flood Protection Structures. Chapter 1 Overview - Studocu." Accessed. Dec. 01, 2025. [Online]. Available. https.//www.studocu.com/row/document/national-university-of-computer-and-emerging-sciences/environmental-engineering/chapter-1-design-criteria/87524544

[12] "USGS Scientific Investigations Report 2009–5262. Conceptual Model of Water Resources in the Kabul Basin, Afghanistan." Accessed. Dec. 01, 2025. [Online]. Available. https.//pubs.usgs.gov/sir/2009/5262/

[13] C. R. W. Zizhan Zhang, B.F. Chao, Jianli Chen, "Terrestrial water storage anomalies of Yangtze River Basin droughts observed by GRACE and connections with ENSO,"

Glob. Planet. Change, vol. 126, pp. 35–45, 2015, doi. https.//doi.org/10.1016/j.gloplacha.2015.01.002.

[14] Ghazala Qaiser, " Climate of Pakistan in 2014," Pakistan Meteorological Department. Accessed. Oct. 27, 2025. [Online]. Available. https.//www.researchgate.net/publication/332269300_Climate_of_Pakistan_in_2014

[15] B. K. Nile, R. J. M. Al-Saadi, L. Abdulameer, N. M. L. Al Maimuri and A. N. Al-Dujaili, "Climate Change Impacts on River Hydraulics. A Global Synthesis of Hydrological Shifts, Ecological Consequences and Adaptive Strategies," *Water Conserv. Sci. Eng.*, vol. 10, no. 2, pp. 1–23, Aug. 2025, doi. 10.1007/S41101-025-00375-Y/METRICS.

[16] J. Sanyal and X. X. Lu, "Application of remote sensing in flood management with special reference to monsoon Asia. A review," *Nat. Hazards*, vol. 33, no. 2, pp. 283–301, Oct. 2004, doi. 10.1023/B.NHAZ.0000037035.65105.95/METRICS.

[17] H. G. Rees and D. N. Collins, "Regional differences in response of flow in glacier-fed Himalayan rivers to climatic warming," *Hydrol. Process.*, vol. 20, no. 10, pp. 2157–2169, Jun. 2006, doi. 10.1002/HYP.6209.

[18] "Rathore on Valuation of Assets." Accessed. Dec. 01, 2025. [Online]. Available. https.//notionpress.com/in/read/rathore-on-valuation-of-assets/